中國機械工程學刊第四十四卷第二期第 109~119 頁(民國一百一十二年)
Journal of the Chinese Society of Mechanical Engineers, Vol.44, No.2, pp109~119 (2023)

Simulation Model and Experimental Verification for Machining of a Horn-shaped Nanochannel

Zone-Ching Lin*, Fang-jung Shiou** ,Yih-Lin Cheng***, Yu-Song Wang*** and Jun-Wei Wen ***

Keywords: horn-shaped nanochannel, atomic force microscopy, two-pass offset machining method

ABSTRACT

The paper develops a simulation model for machining of a horn-shaped nanochannel to the expected width and expected depth. First of all, the paper designs the taper angle of a horn-shaped nanochannel, the opening height and the length of the first cutting pass at the horn-shaped bottom. Then the paper uses two-pass offset machining method. However, the offset amounts between different cutting passes of the oblique line at the horn-shaped side of the horn-shaped nanochannel are different from the offset amount of the horn-shaped middle section. As a result, the upward height value at the bottom of the oblique line at the side would be greater than the upward height value at the bottom of the horn-shaped middle section. Therefore, the paper proposes that for calculation of the number of offset passes and offset amount for machining of a horn shape, the upward height value at the bottom of the oblique side of the horn shape must be smaller than the preset upward height value. 0.54nm at the bottom, but not suggesting that the upward height value at the bottom of the middle section is smaller than 0.54nm. Furthermore, the paper uses specific downward force energy (SDFE) method to calculate the downward force on each cutting layer at each cutting pass, and then simulates calculation of the coordinates of on each cutting layer and each cutting pass of the horn shape in the machining experiment in order to carry out the atomic force microscopic (AFM) machining experiment of the horn shape. The paper also plans the measurement path after the AFM machining experiment. Through comparison between the measurement results of the AFM experiment and the simulation results, the simulation method established by the paper for machining of the horn-shaped nanochannel is proved to be reasonable. The paper proposes using a tiny downward force to conduct straight oblique-line machining along the angle of the horn-shaped oblique side to remove the slightly raised side, making the oblique side become a straight oblique side at a horn-shaped angle.

Paper Received January, 2023. Revised March, 2023. Accepted April, 2023. Author for Correspondence: Zone-Ching Lin

* *Professor, Opto-Mechatronics Technology Center (OMTC), National Taiwan University of Science and Technology, No.43, Keelung Rd., Sec.4, Da'an Dist., Taipei City 10607, Taiwan, email: zclin@mail.ntust.edu.tw.*

** *Professor, Opto-Mechatronics Technology Center (OMTC), National Taiwan University of Science and Technology, No.43, Keelung Rd., Sec.4, Da'an Dist., Taipei City 10607, Taiwan, email: shiou@mail.ntust.edu.tw*

*** *Professor, Department of Mechanical Engineering, National Taiwan University of Science and Technology, No.43, Keelung Rd., Sec.4, Da'an Dist., Taipei City 10607, Taiwan, email: ylcheng@mail.ntust.edu.tw*

*** *Graduated Student, Department of Mechanical Engineering, National Taiwan University of Science and Technology, No.43, Keelung Rd., Sec.4, Da'an Dist., Taipei City 10607, Taiwan, email: m10603211@mail.ntust.edu.tw*

*** *Graduated Student, Department of Mechanical Engineering, National Taiwan University of Science and Technology, No.43, Keelung Rd., Sec.4, Da'an Dist., Taipei City 10607, Taiwan, email: m11003239@mail.ntust.edu.tw*

INTRODUCTION

The paper uses atomic force microscopy (AFM) to machine the microstructure of a horn-shaped nanochannel groove on single-crystal silicon substrate. Regarding application of nanochannel to biomedicine, nanochannels can be used as biosensors, or used for biological screening and testing. Examples of the sensed organisms are bacteria, viruses, and even down to DNA. The paper proposes that the cutting and machining technology that takes AFM probe as a tool for nanochannel-sized machining, can be applied to machining of a horn-shaped nanochannel on the single-crystal silicon substrate surface since this machining method can control its depth and width. Through change of the downward force, the surface roughness at the bottom can be controlled to be flatter than that by etching technology, at the same time achieving the same depth as the etching technology's, so this is really an innovative research.

AFM, invented by Binnig et al. (1986), is a kind of scanning probe microscopy (SPM) commonly applied to measurement and observation of the surface morphology of conductors and non-conductors. Lübben and Johannsmann (2004) saw probe tip as a perfect sphere, and used contact mode AFM to explore the probe deflection and vertical pressure on a quartz plate.Fang et al. (2020) used AFM probe to conduct nano-scratching experiments of silicon (Si) substrate coated with crystal-free aluminum (Al.) film. Experimental results showed that scratch depth deepened with the increase of probe tip load and scribing cycles. Besides, the effects of downward force of the cutting tool of probe were most obvious. Wang et al. (2010) used AFM for machining of nanochannel on the surface of silicon oxide, and explored through experiments how normal force was related to cutting speed and cutting depth. The experiment of scratching Si wafer by AFM cutting tool of probe done by Tseng (2010) also showed that the width and depth of the scratched groove increased with the increase of downward force and scratch cycles of probe. Lin and Hsu (2012) used the theory of specific downward force energy (SDFE) to explore the V-shaped groove produced on the sapphire being cut at different downward forces, and explore the method of reaching the expected machining depth with the fewest cutting passes when machining a V-shaped groove on each cutting layer for a single cutting pass only.Lin et al. (2012) developed a simulation model and equations for machining and integration of two horizontal straight-line nanochannels connected with curved nanochannels and a vertical straight-line nanochannel trapezium groove to the expected width and expected depth, and employed a machining method that used the shape stacking concept and changed the downward force for machining to the expected width and expected depth. Aikawa et al. (2012) carried out cell encapsulation through the polydimethylsiloxane (PDMS) system, which used photolithography to manufacture a horn-shaped nanochannel as well as horizontal and vertical nanochannels. This paper takes the PDMS system as a reference to carry out planning of a horn-shaped nanochannel. In previous literature, the paper's machining method of a horn-shaped nanochannel to the expected width and expected depth has never been mentioned.

EXPERIMENTAL EQUIPMENT AS WELL AS THEORETICAL MODEL AND EXPERIMENTAL METHOD OF SPECIFIC DOWNWARD FORCE ENERGY (SDFE)

Introduction of Experimental Equipment

The AFM machine used in this paper is Veeco Instruments Inc.'s AFM at Dimension 3100 (D3100). The material used in the paper's experiments is silicon substrate with diameter 2 inches and thickness 254-304μm, which was provided by Ample Gola International Co., Ltd. The paper also uses AFM equipment to carry out nanomachining and measurement of surface morphology before and after machining.

The probe used in experiments is the diamond-coated DT-NCHR probe produced by NanoSensors Inc. The thickness of the diamond coating is around 100nm, and the probe tip is like a semi-sphere with a spherical radius of around 150nm. The spring constant k_v of the probe provided by the manufacturer is 42 N/m, and its resonance frequency f_v is 320 kHz. In order to obtain a more accurate spring constant k_r of probe, the paper firstly uses tapping mode AFM to find the actual resonance frequency f_r of probe for experiments. Besides, since the spring constant k_r of probe in the experiments can be obtained from the equation $k_r = (f_r^2 \times k_v)/f_v^2$, the actual spring constant k_r of probe in the experiments can be acquired from the resonance frequency f_v and spring constant k_v of probe provided by the manufacturer, as well as the actually measured resonance frequency f_r. 309.6 kHz.

Measurement Method of Downward Force of AFM Probe

For the nanomachining way by AFM contact mode, the probe firstly presses down into the work-piece. Right now the probe will have deflection. Therefore, downward force is produced in Z axial direction between the probe and the sample. After that, the paper controls the probe to move on the XY plane, and nanomachining can thus be produced. Focusing on the measurement way of downward force of probe onto the workpiece to be machined, this paper uses force-distance curve for measurement. The force-distance curve explains the relationship between set-point value and offset amount of the probe cantilever. Before conducting the experiment, the paper firstly sets different setpoint values for AFM machine under the contact model, and then substitute the offset amount d of probe cantilever measured by different setpoint values in equation (1) to acquire the corre-sponding downward force value F_d of the setpoint. In equation (1), k_r is the spring constant of probe (Digital 3100 Manual,2000)

$$F_d = k_r d \tag{1}$$

SDFE Theoretical Model and SDFE Calculation Method

The paper considers that in the actual nanomachining process, the workpiece is under sufficient downward force from the cutting tool of probe. As downward force energy is produced from pressing downward into the workpiece for a certain depth, machining is carried out in cutting direction. SDFE is defined as follows: Let the downward force of machining applied by the cutting tool of probe onto the workpiece multiply the power of cutting depth to produce energy; and then divide such energy by the volume removed from the workpiece by the cutting tool due to downward force. The equation of SDFE is shown in equation (2) (Lin and Hsu,2012):

$$\text{SDFE (specific downward force energy)} = \frac{F_d \times \Delta d_n}{\Delta V_n} \quad (2)$$

Here, F_d denotes the downward force applied by cutting tool onto the workpiece; Δd_n denotes the increased cutting depth for cutting on the n^{th} layer at the cutting pass; and ΔV_n denotes the volume removed from the cut workpiece at the nth cutting pass. Since the volume cut and removed from the workpiece by downward force changes with the increase of cutting depth, ΔV_n is the function of cutting depth Δd_n. This paper supposes that under the same workpiece material, different downward forces and different cutting passes, the SDFE of nanoscale cutting inclines to be a fixed value.

The cutting at each cutting pass on the 1st cutting layer is just like a semispherical cutting tool pressing into the workpiece to carry out straight-line moving and machining. As observed, after the cutting experiment, from the cross-section morphology of groove depth in cutting direction, the cutting tool of probe initially presses into a shallower depth (Δd_i). As the cutting tool moves, the cutting depth gradually increases from a shallow depth to a fixed value (Δd_1) in the middle area. The removed volume also increases with the deepening of the cutting depth. This phenomenon is the same as the model simulated by the paper using a solid model being actually constructed by CATIA CAD software. Therefore, the paper takes the measured and calculated average cutting depth at the position of middle area of the machined groove as the cutting depth in order to meet the actual machining situation.

As to the volume removed by downward force after moving of cutting tool, due to machining in the abovementioned process, the volume of the distance of the radius R behind the cap of the workpiece being pressed in by the probe in advancing direction has been removed. Therefore, at this moment, the removed volume on the 1st cutting layer at the 1st cutting pass is half of the cap volume under the cutting depth Δd_1, and the removed volume ΔV_1 is shown as follows:

$$\Delta V_1 = \frac{1}{2}\pi \Delta d_1{}^2 \left(R - \frac{\Delta d_1}{3}\right) \quad (3)$$

where R denotes the tip radius of the cutting tool of probe; and Δd_1 denotes the cutting depth on the 1st cutting layer at the 1st cutting pass.

As to the volume removed by downward force on the 2nd cutting layer at the 1st cutting pass, since the groove is removed on the 1st cutting layer at the 1st cutting pass, the removed volume is just like an arc wside. Therefore, for the geometric shape of cutting tool and the cutting depth, the paper uses CATIA's CAD software to make a solid model in order to carry out simulation and calculation of the volume removed by the downward force at 1st cutting pass on the 2nd cutting layer.

TWO-CUTTING-PASS OFFSET MACHINING METHOD OF NANOCHANNEL TRAPEZIUM GROOVE

The paper's two-pass offset machining method of nanochannel trapezium groove is explained as follows: First of all, it is set that under a fixed downward cutting depth on each cutting layer, the cutting depth at the 1st cutting pass is firstly cut. After that, the probe moves a offset amount to cut the workpiece on this cutting layer at the 2nd cutting pass, as shown in figure 1. During this time the cutting depth on this cutting layer at the 2nd cutting pass has the same cutting depth as the 1st cutting pass. In this way, between the shape of the cut cross-section before probe offset and the shape of the cut cross-section of trapezium groove bottom at the two cutting passes after probe offset, there is an upward height value H at the bottom, as shown in Figure 1 (Lin et al, 2022).

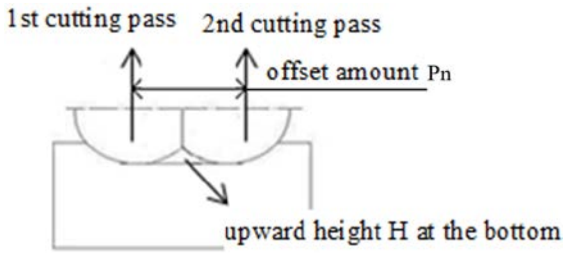

Fig.1. Schematic diagram of upward height value H at the bottom of trapezium groove between two cutting passes

If this upward height value H at the bottom of trapezium groove exceeds the set convergence value of upward height value at the bottom, the probe should be offset step by step to carry out cutting. After step-by-step offset of the probe, the upward height value H at the bottom at the two cutting passes of machining is made to converge to within a range. In order to make the trapezium groove's bottom on the straight-line nanochannel have a result closer to a plane after cutting at the bottom, the paper sets the numerical value of the upward height value at the bottom to be a numerical value of the surface roughness of single-crystal silicon substrate at below 0.54nm. Right now, it is supposed that the probe offset amount required for cutting of nanochannel trapezium groove has been reached. Then, after the probe is offset, substitute the

SDFE value obtained in AFM experiment into the SDFE equation (2).

Since ΔV_n in equation (2) is the function of Δd_n, which is the same cutting depth on this layer at the 1st cutting pass, and the radius of AFM probe has been known, CAD software can be used to find ΔV_n. After inverse induction from equation (2), the required downward force for machining a nano-trapezium groove on this cutting layer at the 2nd cutting pass after probe offset can be acquired.

ESTABLISHMENT OF MACHINING METHOD OF STRAIGHT-LINE NANOCHANNEL TRAPEZIUM GROOVE TO THE EXPECTED DEPTH AND EXPECTED WIDTH

The paper further establishes the method of machining straight-line nanochannel trapezium groove to the expected depth and expected width. The method established in this paper can decide the required number of cutting passes (n) for machining of nanochannel trapezium groove to the expected depth and expected width, total offset amount P_{total} of probe between cutting passes, probe offset amount P_n between two adjacent cutting passes, and the upward height value H at the bottom produced between two adjacent cutting passes. Focusing on this paper's method of machining trapezium groove on straight line segment nanochannel to the expected depth and expected width, the paper further derives the following equations.

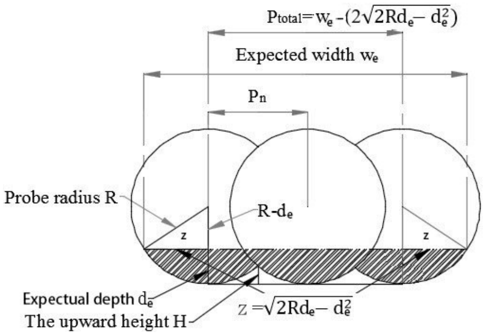

Fig.2. Schematic diagram of geometric relationship in machining of straight-line nanochannel trapezium groove to the expected depth and expected width (3 cutting passes)

First of all, the paper sets the numerical values of the expected depth and expected width for machining the straight-line nanochannel trapezium groove up to the last cutting layer, as shown in Figure 2. Figure 2 is the schematic diagram of machining for 3 cutting passes. In Figure 2, d_e denotes the expected depth of the last straight-line nanochannel trapezium groove; w_e denotes the expected width for machining to the last straight-line nanochannel trapezium groove; P_{total} denotes the total offset amount of probe; P_n denotes the probe offset amount between two adjacent cutting passes; H denotes the upward height value at the bottom; and z denotes the horizontal distance from the center of probe to the connecting place between the probe and the side of trapezium groove. If the probe tip radius R is known, the equation of Pythagorean theorem can be used to derive the equation z in Figure 2, as expressed below (Lin et al.,2022)

$$\because\ z^2 + (\mathrm{R} - d_e)^2 = \mathrm{R}^2$$

$$\therefore\ z = \sqrt{2\mathrm{R}d_e - {d_e}^2} \tag{4}$$

From Figure 2, it can be seen that there is z by both the left and right sides at the farthest cutting pass, so that $2z=2\sqrt{2\mathrm{Rd_e} - \mathrm{d_e}^2}$. In order to obtain the required total offset amount of probe, equation (5) of total offset amount of probe can be derived from Figure 2 as follows:

$$P_{total}= w_e\text{-}(2\sqrt{2\mathrm{R}d_e - {d_e}^2}) \tag{5}$$

As seen from equation (5), when the expected depth and expected width of the last straight-line nanochannel trapezium groove are known, the total offset amount of probe can be acquired from equation (5). During this time, we further find that after calculation of total offset amount of probe, the probe offset amount P_n between two adjacent cutting passes is the main key point affecting the upward height value H at the bottom of the trapezium groove. And from simulation, it is known that if the number of cutting passes in the middle of total offset amount of probe is more, the upward height value H at the bottom will be smaller; and if the number of cutting passes in the middle of total offset amount of probe is less, the upward height value H at the bottom will be greater. When the cutting depth on each cutting layer has been decided, SDFE equation can be used to find the predicted downward force required for reaching the cutting depth on this cutting layer, and then we can decide how much downward force is required when this cutting depth is reached.

The above theoretical equation can be used to derive the required total offset amount of probe. However, how many cutting passes and how much probe offset amount P_n between two adjacent cutting passes should be used are the key questions. If a smaller probe offset amount can be used to reach the expected depth and expected width of the trapezium groove, not only the upward height value at the bottom can be obtained, the number of cutting passes can also be smaller. Therefore, focusing on this point, the paper derives the equation of probe offset amount P_n between two adjacent cutting passes as well as the equation of upward height value H at the bottom between two adjacent cutting passes, as shown in equation (6) and equation (7) respectively below.

As known from Figure 1 and Figure 2, H denotes the upward height value at the bottom of the trapezium groove produced between two adjacent cutting passes; P_n denotes the probe offset amount between two adjacent cutting passes; and the n in P_n denotes the number of cutting passes on each cutting layer. If there are two cutting passes only, the n in P_n is 2, and $P_{total} = P_2$. Therefore, from Figure 1 and Figure 2, the equations of P_n and H can be derived and expressed as equations (6) and (7) as follows:

$$P_n=\frac{P_{total}}{n-1} \tag{6}$$

$$H = R - \sqrt{R^2 - (\frac{P_n}{2})^2} \tag{7}$$

From equation (5), we can calculate the total offset amount P_{total} of probe required for machining of the nanochannel trapezium groove to the expected depth and expected width. If each cutting layer is divided into n cutting passes for cutting, equation (5) can be used to calculate the total offset amount P_{total}. According to equation (6), we can calculate the probe offset amount P_n between two adjacent cutting passes required for the probe to make the trapezium groove reach the expected depth and expected width. After we have obtained the probe offset amount P_n on each cutting layer between two adjacent cutting passes, we also have to substitute this P_n value into equation (7) to calculate the upward height value H at the bottom, and then observe the selected number of cutting passes, and check whether the upward height value H at the bottom has exceeded the convergence value 0.54nm. If the calculated upward height value H at the bottom has exceeded the convergence value 0.54nm, we can add one more cutting pass, and substitute the number of cutting passes n, with a cutting pass additionally increased, into equation (6). Calculate the required probe offset amount P_n, and then observe again whether the upward height value H at the bottom still exceeds 0.54nm. If the upward height value H at the bottom has not exceeded the convergence value 0.54nm, the number of cutting times n set for the new cutting pass is the required number of cutting passes on each cutting layer.

SIMULATION MODEL AND MEASUREMENT VERIFICATION METHOD FOR MACHINING OF A HORN-SHAPED NANOCHANNEL

In previous literature, machining of a horn shape to the expected depth and expected width has never been discussed. Therefore, this paper explores the polydimethylsiloxane (PDMS) system (Aikawa et al., 2012) for machining of a trapezium groove of a horn-shaped nanochannel. The schematic diagram of the nanochannel machined in this paper is shown in Figure 3 below. The known conditions are: the probe radius is 150nm, the length of the 1st cutting pass at the horn-shaped bottom is L_1, the taper angle of the horn shape is θ, the opening height is w_h, and the depth is d. Of them, the depth d is the expected depth in this paper; and the opening height w_h is the expected width in this paper.

Establishment of Theoretical Simulation Model and Machining Method for Machining of the Horn-Shaped Nanochannel to the Expected Width and Expected Depth

Under the known conditions aforesaid, the theoretical simulation steps established by the paper for machining of a horn shape are as follows:

1. As mentioned above, it is known that the preset depth of the horn-shaped nanochannel is d, and the preset width is w_h, so during simulated machining of the horn-shaped nanochannel, the two-pass offset machining method is firstly employed by machining a straight-line segment nanochannel to the expected depth and expected width. Calculate the total offset amount P_{total}, the total number of cutting passes and the offset amount P_n between different cutting passes required for the horn shape with the expected depth and expected width on the middle section of the horn-shaped nanochannel.
2. Figure 4 is the schematic diagram of the results calculated in Step 1, where L_1, L_2, L_3 and L_4 denote the probe moving lengths of different cutting passes, and θ denotes the angle of the horn-shaped nanochannel. In the schematic diagram of Figure 4, it is supposed that there are 4 cutting passes, so that there are 3 offset amounts, P_n. Furthermore, according to equation (8) below, the probe moving lengths of L_1, L_2, L_3 and L_4 are calculated:

   $$L_2 = L_1 - 2 \times P_n \times \tan\theta$$
   $$L_3 = L_2 - 2 \times P_n \times \tan\theta$$
   $$L_4 = L_3 - 2 \times P_n \times \tan\theta \tag{8}$$

   In Figure 4, P_s denotes the length of the connecting line between the ends of the length of each cutting pass when the horn-shaped nanochannel has a taper angle θ. Besides, when we connect the endpoints of the length of each cutting pass, an oblique line L_θ with a taper angle θ would be formed. Here, L_m is the middle section of the horn-shaped nanochannel.
3. After deriving the probe moving length of each cutting pass, the paper uses zig-zag machining method. Suppose that machining starts from the length L_1 of the 1st cutting pass at the horn-shaped bottom, with (x_1, y_1) being the starting point of machining of the 1st cutting pass at the bottom, and (x_2, y_2) being the ending point of machining of the 1st cutting pass at the bottom. Lift the probe and move it up to the starting point (x_3, y_3) of probe machining of the 2nd cutting pass to start machining. Then let the probe carry out machining until the ending point (x_4, y_4) of the 2nd cutting pass. Carry out zig-zag machining in this way until reaching the endpoint (x_8, y_8) of machining length of the last cutting pass. Figure 5 shows the

coordinates of the two endpoints of the length of each cutting pass obtained from the path of the zig-zag machining method aforesaid. In Figure 5, the calculation equations of the coordinates from (x_2,y_2) to (x_8,y_8) are shown in equations (9) below.

$$
\begin{aligned}
(x_2, y_2) &= (x_1 + L_1, y_1)\\
(x_3, y_3) &= (x_2 - P_n \tan\theta, P_n)\\
(x_4, y_4) &= (x_3 - L_2, P_n)\\
(x_5, y_5) &= (x_4 + P_n \tan\theta, 2P_n)\\
(x_6, y_6) &= (x_5 + L_3, 2P_n)\\
(x_7, y_7) &= (x_6 - P_n \tan\theta, 3P_n)\\
(x_8, y_8) &= (x_7 - L_4, 3P_n)
\end{aligned}
\tag{9}
$$

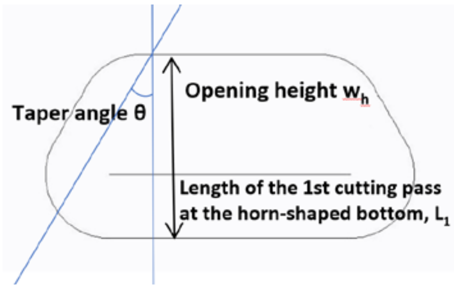

Fig.3. Schematic diagram of a machined horn-shaped nanochannel

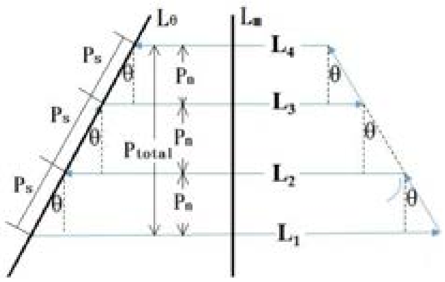

Fig.4. Schematic diagram of total offset amount P_{total} of the horn-shaped nanochannel, number of cutting passes, offset amount P_n between different cutting passes, as well as probe moving length of each cutting pass

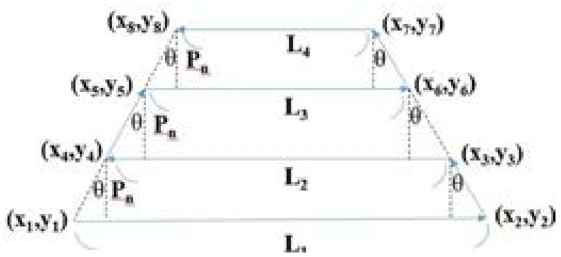

Fig.5. Schematic diagram of the zig-zag machining path of moving probe as well as the coordinates from the starting points to the endpoints of the lengths of different related cutting passes

As shown in Figure 4, on the oblique line L_θ of the horn-shaped nanochannel, since it connects between the endpoints of the length of each cutting pass, the endpoint of the length of each cutting pass is just the starting point or ending point of the moving probe at each cutting pass. Thus, the offset amount at this time is just the length P_s of the oblique line connecting the starting point with the ending point of machining of the lengths at two cutting passes. Therefore, the offset amount P_s at this time can be obtained from equation (10) below. Figure 6 is the schematic diagram of the relationship between P_n and P_s.

After the offset amount P_s of the oblique line is obtained, when the probe intersects the starting point and ending point between the lengths of two cutting passes, an upward height value would be produced at the bottom. At this time the upward height value H_s at the bottom can be calculated by equation (11). Here it should be noted that in Step 1 mentioned above, the offset amount of the middle section of the horn-shaped nanochannel is P_n. Therefore, according to equation (7), the upward height value at the bottom would be: $H = R - \sqrt{R^2 - (\frac{P_n}{2})^2}$. Since the values of H and H_s are different, we can verify in the following steps whether H and H_s are both smaller than 0.54nm.

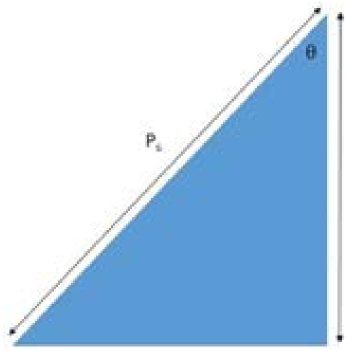

Fig.6. Schematic diagram of the relationship between Pn and Ps

$$P_s = \frac{P_n}{\cos\theta} \tag{10}$$

$$H_s = R - \sqrt{R^2 - (\frac{P_s}{2})^2} \tag{11}$$

4. According to the explanation in the foregoing steps, since it is known from equation (10) that P_s would be greater than P_n, it can be seen from equation (11) that H_s would be greater than H. Therefore, if H is found to be smaller than 0.54nm in the calculation of the number of cutting passes, when H_s is greater than 0.54nm, one more cutting pass must be increased. Then calculation of P_{total}, P_n, P_s, H and H_s should be carried out until H and H_s are both smaller than 0.54nm.

Planning of Path for Removal of the Raised Side of the Horn-Shaped Nanochannel

Regarding the abovementioned machining method of the horn-shaped nanochannel, due to machining of different cutting passes and the shape of the spherical cutting tool, a slightly raised side would be produced on the opening length of the horn-shaped oblique line L_θ of the horn-shaped nanochannel. Figure 8 shows the schematic diagram of the slightly raised side of the horn-shaped nanochannel. Therefore, the paper proposes using a tiny downward force to conduct straight oblique-line machining along the angle of the horn-shaped oblique line L_θ. This tiny downward force would slightly deepen the depth of the side of the straight oblique line. Therefore, the size of the tiny downward force must be controlled well to make the increased depth be smaller than 0.54nm. In this way, the slightly raised side can be removed, and become a straight oblique side. Figure 8 is the schematic diagram of removal of the slightly raised sides of the horn-shaped nanochannel to form straight oblique sides.

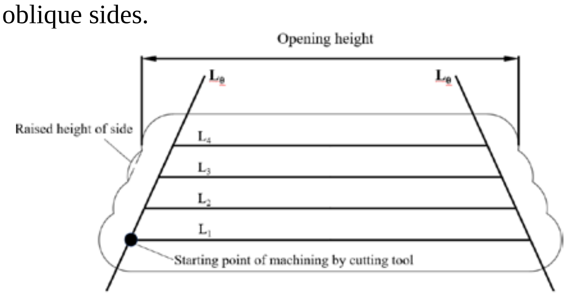

Fig.7. Schematic diagram of the slightly raised sides of the horn-shaped nanochannel

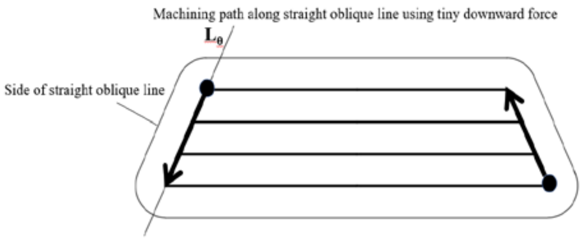

Fig.8. Schematic diagram of removal of the slightly raised sides of the horn-shaped nanochannel to form straight oblique sides

Measurement Verification Method of the Horn-Shaped Nanochannel

In order to verify that the simulation model established by the paper for machining of a horn-shaped nanochannel to the expected width and expected depth is reasonable and acceptable, the paper further establishes the measurement verification method after conducting the AFM machining experiment of the horn-shaped nanochannel. The following measurement verification plan of the horn-shaped nanochannel is explored in 2 steps, as follows:

1. The verification steps of the middle section L_m and the oblique line section L_θ of the horn-shaped nanochannel are as follows:

(1) Take the simulation results of the middle section L_m and the oblique line section L_θ of the horn-shaped nanochannel to carry out verification. Take the measurement sections at the two sections to carry out experimental measurement. Figure 4 has shown the measurement sections of the middle section L_m and the oblique line section L_θ of the horn-shaped nanochannel.

(2) Furthermore, use the aforesaid theoretical simulation model and machining method for machining of the horn-shaped nanochannel to the expected depth and expected width to calculate the simulation results of the total offset amount of the middle section Lm and the oblique line section Lθ, the offset amount of each cutting pass, the number of offset cutting passes, the upward height value at the bottom, the opening height and the expected depth. After that, compare the simulation results with the results measured in the AFM experiment, and then analyze the difference between the simulation and the AFM experiment.

(3) If the difference between the simulation and the experiment is small, and the upward height values at the bottom of the middle section Lm and the oblique line section Lθ of the horn-shaped nanochannel are both smaller than the set target convergence value 0.54nm, then it can be proved that the simulated cutting model established by the paper for machining of the horn-shaped nanochannel to the expected depth and expected width is reasonable.

2. Measurement verification method of the removal of the raised side of the horn-shaped nanochannel as follows:

In order to remove the slightly raised side, the paper proposes using a tiny downward force to carry out straight oblique-line machining along the angle θ of the horn-shaped oblique line. This act can remove the slightly raised side. The paper further plans the measurement verification by measuring the raised side. For the 3 measurement sections being used, 3 lengths are measured first. It is found that after machining with a tiny downward force, the raised side of the horn-shaped oblique line can be removed, making the oblique line become a straight oblique line at a horn-shaped angle. Besides, make measurement after cutting on the oblique line section L_θ, and the increased depth is confirmed to be less than 0.54nm, proving that the method proposed by the paper is feasible.

Measurement verification steps of the removal of the raised side are as follows:

(1) Carry out measurement of the 3 measurement sections of Lm1, Lm2 and Lm3 shown in Figure 9. Of them, Lm1 and Lm2 are the straight lines formed by the low points of the simulated raised side, and Lm2 is the straight line formed by the high points of the raised side. According to the points of intersection between the simulated straight lines Lm1, Lm2 and L_{m3}, and the two raised sides of the horn-shaped nanochannel, the equations of the straight line L_{m1}, L_{m2} and L_{m3} can be calculated and expressed as equations (12), which are shown as follows:

L_{m1} is $y_{m1} = a_{m1}x_{m1} + b_{m1}$

L_{m2} is $y_{m2} = a_{m2}x_{m2} + b_{m2}$

L_{m3} is $y_{m3} = a_{m3}x_{m3} + b_{m3}$ (12)

In the above equations, y_{m1} and x_{m1} denote the points of intersection between L_{m1} and the low points of the two raised sides of the horn-shaped nanochannel; y_{m2} and x_{m2} are the points of intersection between L_{m2} and the high points of the raised sides of the horn-shaped nanochannel; and y_{m3} and x_{m3} are the points of intersection between L_{m3} and the low points of the two raised sides of the horn-shaped nanochannel.

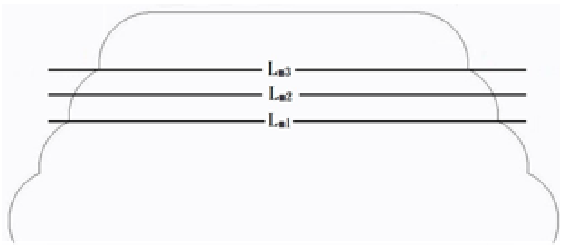

Fig.9. Schematic diagram of 3 measurement sections of the horn-shaped nanochannel

Carry out measurement of the aforesaid 3 measurement sections of L_{m1}, L_{m2} and L_{m3}. According to the points of intersection between the simulated straight lines L_{m1}, L_{m2} and L_{m3}, and the horn-shaped nanochannel's straight oblique lines and two raised sides, the equations of the straight lines L_{m1}, L_{m2} and L_{m3} can be calculated and expressed as equations (12).

In the above equations, y_{m1} and x_{m1} denote the points of intersection between the section straight line L_{m1} and the raised side of the straight oblique line after simulated removal of the raised side; y_{m2} and x_{m2} are the points of intersection between the section straight line L_{m2} and the side of the straight oblique line after simulated removal of the raised side; and y_{m3} and x_{m3} are the points of intersection between the section straight line L_{m3} and the side of the straight oblique line after simulated removal of the raised side.

Using the aforesaid 3 measurement sections L_{m1}, L_{m2} and L_{m3}, and using AFM to measure these 3 sections, the points of intersection between L_{m1}, L_{m2} and L_{m3} and the horn-shaped nanochannel can be obtained. Through the obtained points of intersection, the lengths of l_{m1} , l_{m2} and l_{m3} formed by the points of intersection between the straight oblique sides of the horn-shaped nanochannel and L_{m1}, L_{m2} and L_{m3} can be measured.

(2) Compare the simulation and experimental results. Then it can be proved that the simulation model established by the paper for removal of the raised side of the horn-shaped nanochannel is reasonable.

MACHINING AND SIMULATION RESULTS AND EXPERIMENTAL VERIFICATION OF THE HORN-SHAPED NANOCHANNEL

In order to prove the feasibility of the theoretical model for simulation of machining of the horn-shaped nanochannel mentioned in the previous paragraph, this paragraph takes a 30º horn-shaped nanochannel being machined to the expected depth 30nm and expected width 250nm for 5 cutting passes, as an example to give explanation. According to the calculation steps stated in the previous paragraph, the coordinates of the expected width and expected depth that the horn-shaped nanochannel is machined to can be calculated. Since the smallest resolution achieved by AFM machine is up to 1nm only, the numerical value of the line segment with a decimal point is rounded to an integer value with a precision of 1nm, as shown in Figure 10 below:

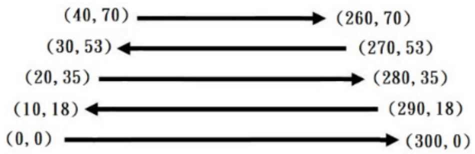

Fig.10. Coordinates of the expected depth 30nm and expected width 250nm in 5 cutting passes

After that, carry out calculation of the measurement section after the AFM machining experiment. According to the verification method and steps mentioned in the previous paragraph, take a measurement section at the measurement section of L_m; take a measurement section at the measurement section of the oblique line L_θ; and take 3 measurement sections of L_{m1}, L_{m2} and L_{m3} at the measurement side section. After calculation, the equations of straight lines of the measurement sections are obtained: L_m is $y_m = x + 300$, L_θ is $y_\theta = 1.7318x_\theta + 0.0087$, L_{m1} is $y_{m1} = x_{m1} + 500$, L_{m2} is $y_{m2} = x_{m2} - 500$, and L_{m3} is $y_{m3} = -x_{m3} + 500$.

After obtaining the various equations of measurement sections aforesaid, we can start to carry out verification of the simulation results and experimental results of machining of the 30º horn-shaped nanochannel to the expected depth and expected width.

Measurement Verification of Simulation Results and Experimental Results of Machining of a 30º Horn-Shaped Nanochannel to the Expected Depth 30nm and Expected Width 250nm for 5 Cutting Passes

The paper carries out simulation of machining of a 30º horn-shaped nanochannel to the expected depth 30nm and expected width 250nm for 5 cutting passes, and obtains the width, depth and upward height value at the bottom of each cutting pass and on each cutting layer. The paper also carries out measurement verification of the AFM experiment, and compares the simulation with the AFM machining experimental measurement, as shown in Table 1 below.

Table 1. Comparison between simulation and experimental results of the 2nd cutting layer of a 30º horn-shaped nanochannel being machined to the expected depth 30nm and expected width 250nm for 5 cutting passes

2nd Layer	Downward force (μN)	Cutting pass	Experimental cutting depth (nm)	Simulated cutting depth (nm)	Difference in cutting depth (%)	Offset amount (nm)	Experimental upward height value (nm)	Simulated upward height value (nm)	Difference in upward height value (%)	SDFE VALUE	Experimental opening width (nm)	Simulated opening width (nm)	Difference in opening width (%)
Measurement section of L_m	34.10	1st cutting pass	30.019	30.000	0.063%	17.500	0.249	0.255	2.35%	0.01775	250.046	250.009	0.015%
	15.36	2nd cutting pass	30.019	30.000	0.063%	17.500	0.249		2.35%	0.01775			
		3rd cutting pass	30.019	30.000	0.063%	17.500	0.249		2.35%	0.01775			
		4th cutting pass	30.019	30.000	0.063%	17.500	0.249		2.35%	0.01775			
		5th cutting pass	30.019	30.000	0.063%					0.01775			
Measurement section of L_θ	34.10	1st cutting pass	30.019	30.000	0.063%	20.207	0.332	0.340	2.50%	0.01775	274.783	274.747	0.013%
	15.36	2nd cutting pass	30.019	30.000	0.063%	20.207	0.332		2.50%	0.01775			
		3rd cutting pass	30.019	30.000	0.063%	20.207	0.332		2.50%	0.01775			
		4th cutting pass	30.019	30.000	0.063%	20.207	0.332		2.50%	0.01775			
		5th cutting pass	30.019	30.000	0.063%					0.01775			

From Table 1, the difference between the simulation and experimental results can be seen. The values of difference in depth are all smaller than 0.08%, and the values of difference in width are all smaller than 0.015%. The upward height values at the bottom of measurement sections of L_m and L_θ are all smaller than the target convergence value 0.54nm. Therefore, it can be proved that the simulation method proposed by the paper for machining of a 30º horn-shaped nanochannel is feasible. Figure 11 to Figure 13 below show the diagrams of part of the AFM experimental measurement results, proving that the experimental data in Table 1 above are obtained from the AFM experimental measurements.

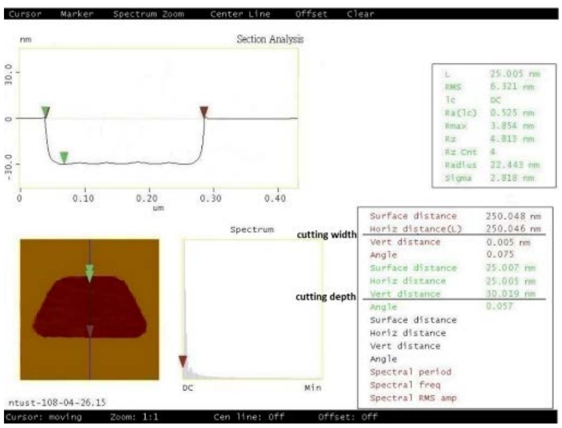

Fig.11. Diagram of measurement of the opening width and cutting depth of measurement section of L_m on the 2nd cutting layer of a 30º horn-shaped nanochannel being machined to the expected depth 30nm and expected width 250nm for 5 cutting passes

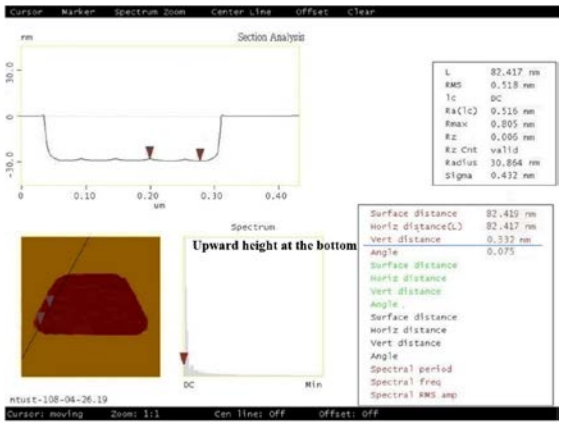

Fig.12. Diagram of measurement of upward height values of measurement section of L_θ on the 2nd cutting layer of a 30º horn-shaped nanochannel being machined to the expected depth 30nm and expected width 250nm for 5 cutting passes

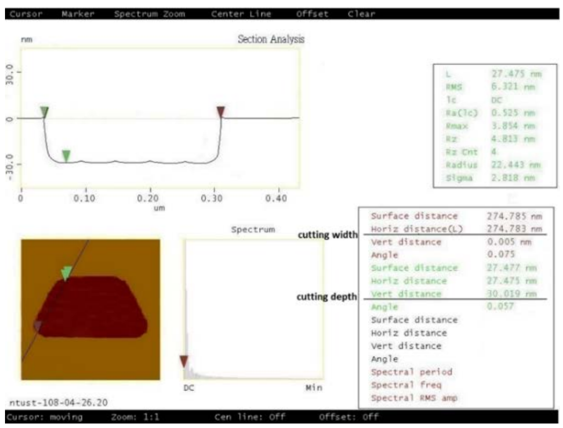

Fig.13. Diagram of measurement of the opening width and cutting depth values of measurement section of L_θ on the 2nd cutting layer of a 30° horn-shaped nanochannel being machined to the expected depth 30nm and expected width 250nm for 5 cutting passes

Analysis of Simulation Results and Experimental Results of Removal of the Slightly Raised Sides of the 30° Horn-Shaped Nanochannel

The paper follows the cutting path for removing the slightly raised side planned by the paper above that a smaller downward force 2.81μN is used to carry out cutting along the horn-shaped oblique line L_θ. As mentioned above, 3 measurement section lengths (l_{m1}, l_{m2} and l_{m3}) are obtained. The paper makes comparison between the simulation and experimental results, and finally measures the cutting depth after confirmed cutting of the measurement section of L_θ. After cutting, the depth increases from the original 30.019nm to be 30.248nm, which meets the theoretical model's rule that the increased depth must not exceed 0.54nm. Then it can be proved that the simulation model and experimental method established by the paper for removal of the slightly raised side of the horn-shaped nanochannel is feasible.

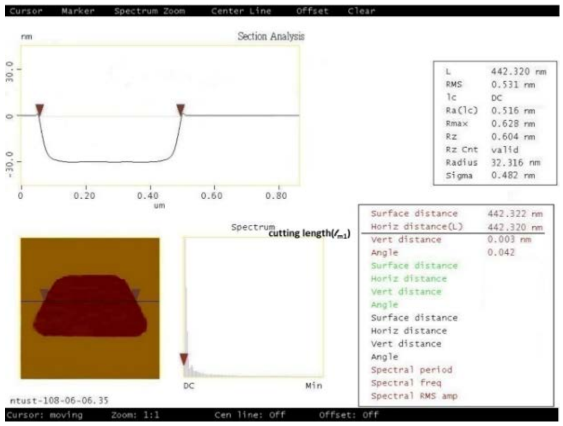

Fig.14. Diagram of measurement for removal of the slightly raised sides ℓ_{m1} of the 30° horn-shaped nanochannel being machined to the expected depth 30nm and expected width 250nm for 5 cutting passes

Table 2 shows the simulation and experimental data on the measurement section lengths (l_{m1} and l_{m2} and l_{m3}) and removal of the slightly raised sides. The values of difference in cutting depth are all smaller than 0.024%. Figure 14 shows the diagrams of part of the AFM experimental measurement results, proving that the experimental data in Table 2 are obtained from the AFM experimental measurements.

Table 2. Simulation and experimental data for removal of the slightly raised sides of the 30° horn-shaped nanochannel being machined to the expected depth 30nm and expected width 250nm for 5 cutting passes

Removal of the slightly raised side	Experimental cutting length (nm)	Simulated cutting length (nm)	Difference in cutting length (%)
Measurement section length ℓ_{m1}	442.320	442.214	0.024%
Measurement section length ℓ_{m2}	439.695	439.590	0.024%
Measurement section length ℓ_{m3}	439.471	439.366	0.024%

CONCLUSION

The paper proposes the simulation model and method for machining of a horn-shaped nanochannel to the expected width and expected depth. Using the established simulation model, the paper preliminarily calculates the total offset amount for the height of the opening to be machined, the number of cutting passes and the upward height value at the bottom. Finally, using the maximum downward force allowed by the probe, the paper calculates the number of cutting layers. Also using the simulated and calculated downward force on each cutting layer at each cutting pass, the paper applies these calculated data to the machining of the horn-shaped nanochannel. Besides, in order to improve the situation that a slightly raised side is produced from machining by the spherical cutting tool during machining of the nanochannel, the paper employs a method by applying a smaller downward force on the slightly raised side and using a planned method with an increased removal of the slightly raised side along the machining path, thus making the nanochannel flatter. The paper also proposes a measurement verification method by using AFM experiment for machining of the horn-shaped nanochannel. After comparison is made between the simulation results and the AFM experimental results, it is proved that the simulation model established by the paper for machining of a horn-shaped nanochannel to the expected width and expected depth is reasonable and acceptable.

ACKNOWLEDGEMENT

The authors would like to thank the support from National of Science and Technology Council, Taiwan. (MOST 111-2221-E-011-101-)

REFERENCES

Aikawa, T., Konno, T., Takai, M. and Ishihara, K., "Spherical Phospholipid Polymer Hydrogels for

Cell Encapsulation Prepared with a Flow-Focusing Microfluidic Channel Device", ACS Journal of American Chemical Society, Vol. 28, No. 3, pp. 2145-2150 (2012).

Binning, G., Quate, C. F. and Gerber, C., "Atomic Force Microscope", Physical Review Letters, Vol. 56, No. 6, pp. 930-933 (1986).

Digital Instruments Dimension™ 3100 Manual. Version 4.43B, Digital Instruments Veeco Metrilogy Group (2000).

Fang, T. H., Weng, C. I. and Chang, J. G., "Machining Characterization of Nano-lithography Process by Using Atomic Force Microscopy", Nanotechnology, Vol. 11, No. 5, pp. 181-187 (2000).

Lin, Z. C. and Hsu, Y. C., "A calculating method for the fewest cutting passes on sapphire substrate at a certain depth using specific down force energy with an AFM probe", Journal of Materials Processing Technology, Vol. 212, pp. 2321-2331 (2012).

Lin, Z. C., Ho, J. M., & Chen, Z. R., "Machining Simulation Model of Integration of Two Horizontal Straight-line Connected with Curved and Vertical Straight-line Nanochannel as well as Experimental Verification by Atomic Force Microscopy", Journal of the Chinese Society of Mechanical Engineers, Vol. 43, No. 4, pp. 295-306 (2022).

Lübben, J. F. and Johannsmann, D., "Nanoscale High-frequency Contact Mechanics Using an AFM Tip and a Quartz Crystal Resonator", Langmuir, Vol. 20, No. 9, pp. 3698-3703 (2004).

Nanjo, H., Nony, L., Yoneya, M. and Aime, J. P., "Simulation of Section Curve by Phase Constant Dynamic Mode Atomic Force Microscopy in Non-contact Situation", Applied Surface Science, Vol. 210, No. 1, pp. 49-53 (2003).

Tseng, A. A., "A comparison study of scratch and wear properties using atomic force microscopy", J. Applied Surface Science, Vol. 256, Issue 13, pp. 4246- 4252 (2010).

Wang, Z. Q., Jiao, N. D., Tung, S. and Dong, Z. L., "Research on the atomic force microscopy-based fabrication of nanochannels on silicon oxide surfaces", Chinese Science Bulletin, Vol. 55, No. 30, pp. 3466-3471 (2010).

Yongda, Y., Tao, S., Liang, Y. C. and Shen, D., "Investigation on AFM based micro/nano CNC machining system", International Journal of Machine Tools and Manufacture, Vol. 47, No. 11, pp.1651-1659 (2007).

加工喇叭型奈米流道之模擬模式及實驗驗證

林榮慶 修芳仲
國立台灣科技大學 光機電技術研發中心

鄭逸琳 王昱菘 温俊瑋
國立台灣科技大學 機械工程系

摘要

本文提出喇叭型奈米流道加工到預定寬度及預定深度之模擬模式，本文先設計喇叭型奈米流道的推拔角、開口高度以及喇叭型底部的第一切削道次的長度，再利用兩道次偏移加工法。又因為喇叭型奈米流道的喇叭型邊緣的斜線的各切削道次間之偏移量會和喇叭型中間斷面的偏移量不同，造成邊緣斜線的底部上凸值會大於喇叭型中間斷面的底部上凸值。因此本研究提出計算喇叭型的加工偏移道次及偏移量，要以喇叭型斜邊邊線的底部上凸值要小於所設定的底部上凸值 0.54nm，而不是以中間斷面的底部上凸值小於 0.54nm 為主。本研究再進一步用比下壓能法，計算出各切削層的各切削道次的下壓力，再模擬計算喇叭型的各切削層及各切削道次的加工實驗座標點來進行 AFM 喇叭型加工實驗，本文並規劃 AFM 加工實驗後的量測路徑，將 AFM 實驗量測結果與模擬結果做比較，以驗證本文所建立模擬加工喇叭型奈米流道的方法為合理的。故本文提出用一微小下壓力沿著喇叭型斜邊的角度進行斜直線加工，則可清除微小凸起的側邊，使斜邊成為喇叭型的角度直斜邊，且因微小下壓力產生的下凹深度也會小於 0.54nm